OPEN

NPG Asia Materials (2018) 10, e466; doi:10.1038/am.2017.238
www.nature.com/am

ORIGINAL ARTICLE

Selective fabrication of free-standing ABA and ABC trilayer graphene with/without Dirac-cone energy bands

Katsuaki Sugawara[1,2], Norifumi Yamamura[3], Keita Matsuda[4], Wataru Norimatsu[4], Michiko Kusunoki[5], Takafumi Sato[2,3] and Takashi Takahashi[1,2,3]

Graphene is a single-layer carbon sheet with a honeycomb structure, and bilayer graphene consists of two graphene sheets with AB stacking. In trilayer graphene, the third graphene sheet has two possible stacking sequences, A or C, when it is overlaid on bilayer graphene. It has been theoretically predicted that trilayer graphene exhibits a variety of novel electronic properties with/without a Dirac-cone band, depending on the stacking sequence. In this regard, trilayer graphene has a high potential for widening the capability of graphene-based electronic devices. However, the difficulty of selective fabrication has hindered the progress of research. Here, we report the first success in the selective fabrication of quasi-free-standing trilayer graphene with ABA or ABC stacking grown epitaxially on hydrogen-terminated silicon carbide. Angle-resolved photoemission spectroscopy (ARPES) clearly demonstrated that our trilayer graphene with ABA stacking has a massless Dirac-like band near the Fermi level, while that with ABC stacking shows a parabolic non-Dirac-like band dispersion.
NPG Asia Materials (2018) **10,** e466; doi:10.1038/am.2017.238; published online 9 February 2018

INTRODUCTION

Controlling the stacking sequence of layered materials is a useful approach to realizing exotic physical properties and novel electric devices, as observed in the drastically different physical properties between the 1*T*- and 2*H*-phases of transition-metal dichalcogenides.[1–5] Graphite—multilayer graphene with a honeycomb lattice network of carbon atoms—is perhaps the most famous representative of layered materials and has been a target of intensive studies for more than a century.[6] Owing to the weak van der Waals coupling between adjacent layers, graphite has several different forms depending on its crystallinity, such as highly oriented pyrolytic graphite (HOPG), natural graphite and kish graphite (artificial single-crystal graphite). While HOPG has no specific stacking sequence, natural and kish graphite are mainly composed of AB-stacking layers (Bernal structure)[7] with some admixture from ABC stacking (rhombohedral structure).[8] It has long been empirically known that realizing a purely ABC-stacking phase is extremely difficult despite the fundamental interest in its expected peculiar properties because the ABC-stacking phase is relatively unstable. In this regard, trilayer (TL) graphene serves as a useful platform for studying the relationship between stacking sequence and physical properties, as it is the thinnest (and therefore the simplest) unit for realizing ABC stacking.

It is known that, compared with TL graphene, monolayer (ML) and bilayer (BL) graphene can be obtained more easily using various techniques such as exfoliation and epitaxial methods. Intensive studies on ML and BL graphene have clarified a close relationship between their electronic and physical properties. For example, in ML graphene, the massless Dirac-cone state with a linear band dispersion around the K point leads to the integer quantum Hall effect[9] and the valley filter effect,[10] while bilayer graphene with AB stacking can be used as a semiconductor device by utilizing the gapped Dirac cone under an external electric field.[11,12] On the other hand, experimental investigation of trilayer graphene is relatively scarce, partially because of the difficulty in selectively obtaining two different types of TL graphene, that is, ABA and ABC type (Figures 1a and b). Band-structure calculations have predicted that the electronic states of TL graphene strongly depend on the stacking sequence.[13,14] As shown in Figures 1c and d, TL graphene with ABA stacking (called ABA graphene) features three bands near E_F, two of which cross the Fermi level (E_F) at the K point. Importantly, the inner band shows massless Dirac-fermion-like behavior with a linear energy dispersion around E_F. In contrast, in TL graphene with ABC stacking (ABC graphene), a parabolic band touches E_F at the K point.[13] It was theoretically proposed that applying an external electric field leads to energy-gap opening in ABC graphene, while a finite density of states (DOS) persists at E_F in ABA graphene due to the hybridization between the inner and outer bands.[13] Such characteristic band dispersions and physical properties of TL graphene have been recently examined by optical and magneto-transport measurements of ABA and/or ABC graphene obtained by mechanical exfoliation. These studies have revealed the emergence/absence of a predicted energy gap under the application of electric field and the unusual quantum Hall effect.[15–17]

[1]WPI-Advanced Institute for Materials Research, Tohoku University, Sendai, Japan; [2]Center for Spintronics Research Network, Tohoku University, Sendai, Japan; [3]Department of Physics, Tohoku University, Sendai, Japan; [4]Department of Materials Chemistry, Graduate School of Engineering, Nagoya University, Nagoya, Japan and [5]Institute of Materials and Systems for Sustainability, Nagoya University, Nagoya, Japan
Correspondence: Professor T Takahashi, WPI-AIMR, Tohoku University, Katahira 2-1-1, Aoba-ku, Sendai 980-8577, Japan.
E-mail: t.takahashi@arpes.phys.tohoku.ac.jp.
Received 3 July 2017; revised 28 November 2017; accepted 29 November 2017

To further investigate the essential difference in the electronic states between two types of TL graphene and to realize feasible TL-graphene-based devices, it is of great importance to selectively fabricate free-standing ABA and ABC graphene with a large terrace size by the epitaxial technique. Although epitaxial graphene has several advantages in practical applications because of the precise controllability of the stacking sequence, selective fabrication via the epitaxial method has not been feasible to date. In fact, previous angle-resolved photoemission spectroscopy (ARPES) studies on epitaxially grown TL graphene have suggested the mixture of ABA and ABC domains in a film.[18–20] In addition, TL graphene grown on an SiC substrate exhibits a metallic character because of charge transfer from the substrate through a buffer layer with a graphene-like structure.[15] Therefore, graphitization of the buffer layer and the reduction of interference from the substrate are essential to revealing the intrinsic electronic properties of genuine TL graphene. Here, we report the first success in the selective fabrication of quasi-free-standing ABA and ABC TL-graphene epitaxial films on hydrogen-terminated SiC and their characterization using ARPES and transmission electron microscopy (TEM).

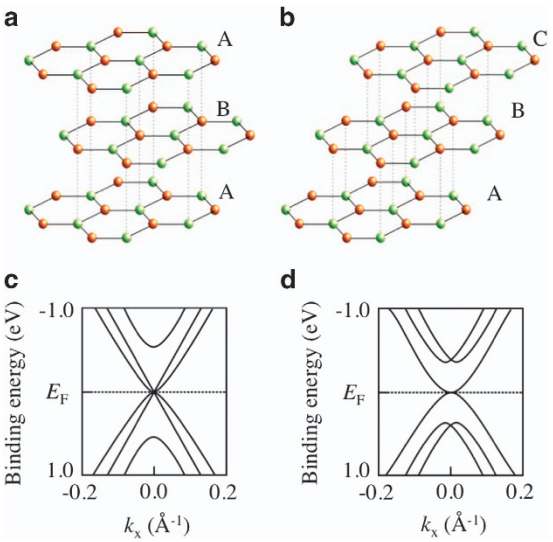

Figure 1 Crystal and electronic structures of trilayer graphene with ABA and ABC stacking. (**a** and **b**) Crystal structure of TL graphene with (**a**) ABA and (**b**) ABC stacking. (**c** and **d**) Calculated band structure around the K point for (**c**) ABA and (**d**) ABC TL graphene.[13,19]

METHODS

ARPES measurements were performed using an Omicron-Scienta SES2002 electron analyzer with a high-flux helium discharge lamp and a toroidal grating monochromator. We used the He IIα (40.814 eV) resonance line to excite photoelectrons. The energy and angular resolutions were set to 16 meV and 0.2°, respectively. High-resolution TEM measurements were carried out on a JEM-2010F-type microscope at an accelerating voltage of 200 kV.

RESULTS AND DISCUSSION

First, we explain how quasi-free-standing TL graphene is selectively fabricated. We first prepared BL graphene with a buffer layer by annealing *n*-type Si-terminated 6*H*-SiC(0001)[18,21,22] under two different experimental conditions. For ABA graphene, we annealed SiC at 1510 °C under a 0.1 MPa Ar atmosphere, while for ABC graphene we annealed SiC at 1300 °C in a high vacuum of $\sim 1.0 \times 10^{-7}$ Torr. It should be

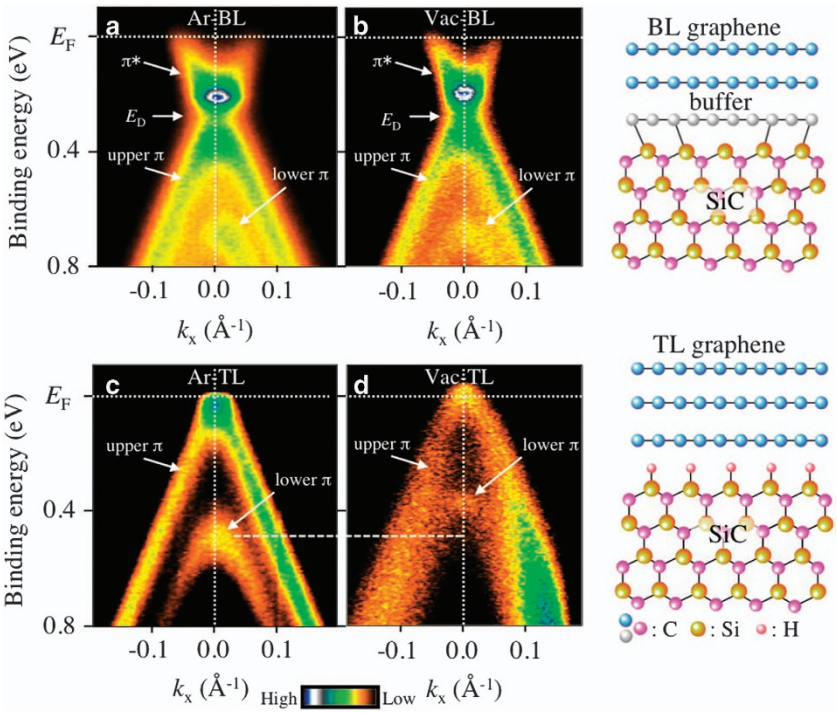

Figure 2 Dirac and non-Dirac dispersions in ABA and ABC trilayer graphene. (**a** and **b**) ARPES-derived band dispersions near E_F around the K point of BL graphene with buffer layer on SiC(0001) fabricated by keeping the substrate (**a**) at 1510 °C under 0.1MPa Ar atmosphere (labeled Ar-BL graphene) and (**b**) at 1300 °C in a vacuum of $\sim 1.0 \times 10^{-7}$ Torr (labeled Vac-BL graphene). (**c** and **d**) Same as (**a** and **b**), but for quasi-free-standing TL graphene obtained by spraying hydrogen atoms onto samples. Right upper and lower panels show the schematic illustration of BL graphene with buffer layer on SiC and TL graphene on SiC after hydrogen termination, respectively. The band dispersion in (**a**–**c**) was obtained at $T = 30$ K, while that in (**d**) was at $T = 300$ K to visualize more clearly the parabolic band dispersion above E_F by using the thermal broadening.

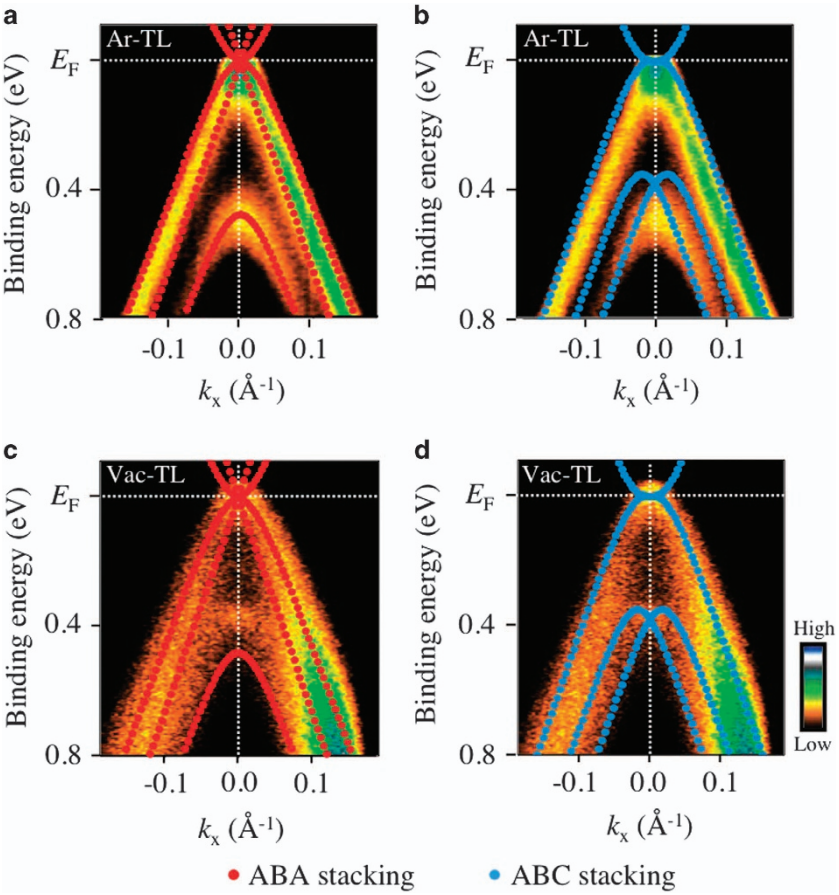

Figure 3 Comparison of band dispersions near the Fermi level between experiment and calculation for ABA and ABC trilayer graphene. (**a** and **b**) ARPES-derived band dispersions near the Fermi level for Ar-TL graphene compared with the tight-binding calculations for (**a**) ABA and (**b**) ABC graphene, respectively, performed by referring to refs. 25 and 26. (**c** and **d**) Same as (**a** and **b**) but for Vac-TL graphene. The hopping parameters (γ_0, γ_1, γ_3) in the calculations[25,26] are set at (–3.12, –0.34, –0.24) (in eV unit) for ABA graphene and (–3.12, –0.38, –0.24) for ABC graphene. Comparison of these values suggests that γ_1 slightly depends on the stacking sequence.

noted that this precise temperature and pressure control is the key to selectively fabricating ABA and ABC phases. We then sprayed 'cracked' hydrogen gas onto the as-grown BL graphene film in a vacuum of 1.0×10^{-3} Torr by keeping the substrate at 500 °C. The duration of hydrogen gas flow was 120 min. The cracking of hydrogen molecules into hydrogen atoms was performed by a tungsten filament heated to 1600 °C[22,23] in front of the BL graphene sample. This hydrogenation process terminates chemical bonding from the SiC substrate and simultaneously converts the buffer layer into a single graphene layer, leading to the formation of quasi-free-standing TL graphene.[19,22–24]

Figures 2a and b show a side-by-side comparison of the band dispersion near E_F around the K point obtained by ARPES between two BL graphene samples prepared under different experimental conditions. BL graphene, labeled 'Ar-BL' (Figure 2a), was prepared under an Ar atmosphere, while that labeled 'Vac-BL' (Figure 2b) was obtained under high vacuum as previously described. It is noted that both BL graphene samples are on a buffer layer at this stage (see the schematic illustration in the right panel of Figure 2). As shown, the observed band structures are very similar to each other despite the very different sample-growth conditions. For example, two π bands with the top of the dispersion at binding energies (E_B) of ~0.4 and ~0.7 eV (upper and lower π bands, respectively), as well as a π* band with the bottom at ~0.2 eV, are observed in both samples. The Dirac point E_D defined as the midpoint of the π*-band bottom and the π-band top is located at $E_B \sim 0.35$ eV, suggesting charge (electron) transfer from the substrate through the buffer layer.

Figures 2c and d show the band dispersion near E_F after hydrogenation. One can immediately recognize that the π bands are pushed upward, leaving no signature of the π* band. Additionally, the Dirac point is moved to E_F. This change in the electronic structure suggests that hydrogenation suppresses charge transfer from the substrate, and the buffer layer is graphitized to form quasi-free-standing TL graphene, as schematically illustrated in the right panel of Figure 2.[19,22,24] However, despite the similar upward shift in overall band dispersion, we find several interesting differences between Ar-TL graphene (Figure 2c) and Vac-TL graphene (Figure 2d). First, the upper π band in Ar-TL graphene appears to show a straight dispersion, as in the case of a Dirac cone in free-standing ML graphene (the Fermi velocity is estimated to be 5.7 eVÅ (8.7×10^5 m s^{-1}) by linear extrapolation of bands), while that in Vac-TL graphene is apparently 'rounded' near E_F and is not Dirac-cone-like. Second, the top of the lower π band in Ar-TL graphene (indicated by horizontal dashed line) is located at $E_B \sim 0.5$ eV, while that of Vac-TL graphene is observed at $E_B \sim 0.4$ eV. These differences suggest that TL graphene samples fabricated under two different conditions should be fundamentally different from each other.

To understand the origin of such differences, we compare the ARPES-derived band dispersion of Ar-TL graphene with the band

structure calculated for ABA and ABC graphene by using the tight-binding model[25,26] in Figures 3a and b, respectively. The straight feature of upper π band observed in the experiment shows better agreement with the calculated band for ABA graphene than that for ABC graphene (note that the ARPES data do not resolve the inner and outer bands in calculated ABA graphene, likely because of the finite resolution and quasiparticle scattering effects). Moreover, the experimental dispersion of the lower π band is reproduced well by the calculation for ABA graphene. On the other hand, when we compare the ARPES result for Vac-TL graphene with the calculated bands in a similar manner (Figures 3c and d), we immediately recognize that the overall experimental band dispersion nicely overlaps with the calculated bands for ABC graphene, as indicated by the rounded shape of the upper π band and the location of the lower π band. These results strongly suggest that Ar-TL and Vac-TL graphene are attributed to ABA and ABC graphene, respectively. It is noted that if the contribution of ABA stacking is combined with the ARPES intensity of the fabricated ABC graphene sample, one would expect to observe a subpeak structure at 0.5 eV at the K point arising from the top of the lower π band. We carefully examined this possibility by analyzing the energy distribution curve at the K point and found no clear evidence for such a subpeak. This result suggests that, while it is difficult to completely rule out the possibility of a finite admixture of other stacking sequences, their volume fraction is likely less than a few percent with respect to that of ABC stacking. We emphasize here that ABA graphene is generally more stable than ABC graphene,[8,27] and previous ARPES studies of TL graphene have mainly focused on the electronic states of ABA graphene.[18] In contrast, in this study, we succeeded in fabricating unstable ABC graphene by precisely tuning the sample-growth conditions and revealed the differences/similarities between ABA and ABC graphene.

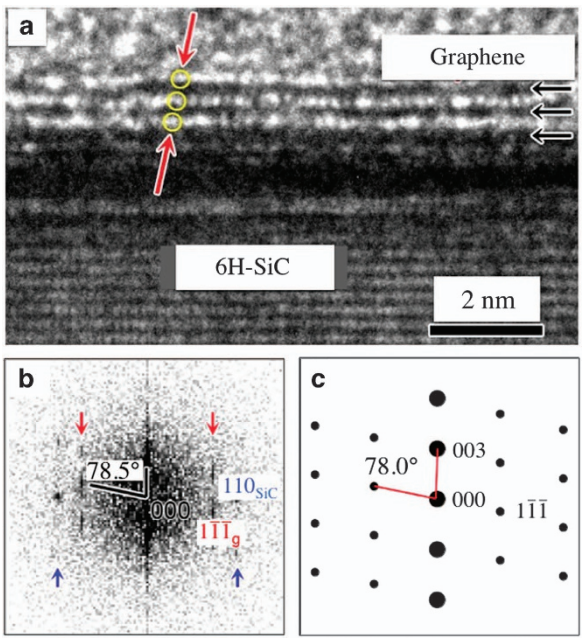

Figure 4 Characterization of stacking order in ABC trilayer graphene by TEM. (**a**) High-resolution TEM image of Vac-TL graphene. Incident electron beam is parallel to the $(11\bar{0}0)_{SiC}$ direction. Yellow circles indicate the stacking sequence of graphene layers. (**b**) FFT pattern obtained from the TEM image. Diffraction spots indicated by red and blue arrows correspond to TL graphene and SiC, respectively. (**c**) Simulated FFT pattern for ABC TL graphene.[28]

To further examine the validity of our assignment on the ABC nature of Vac-TL graphene, we performed high-resolution TEM measurements for Vac-TL graphene. As shown in the TEM image (Figure 4a), three well-resolved graphene layers are systematically piled on the 6H-SiC substrate, confirming that our graphene film is indeed TL graphene. Additionally, as indicated by yellow circles, carbon atoms are arranged such that they are slightly slanted relative to the normal of the graphene plane, indicative of ABC stacking. Figure 4b shows the fast-Fourier transform (FFT) pattern obtained from the TEM image (Figure 4a), which is equivalent to the electron diffraction pattern. The several sharp spots observed in the FFT pattern indicate the existence of long-range periodicity in the arrangement of carbon atoms. As shown in Figure 4b, the angle between the line connecting the 003 and 000 spots and the line connecting the 111 and 000 spots is ~78.5°. This value is in good agreement with that estimated from the simulated FFT pattern for ABC graphene (78.0°) (Figure 4c),[28] confirming that graphene sheets in our Vac-TL graphene are stacked in the ABC sequence. It is noted that the TEM image shows a dark gap between SiC and trilayer graphene. This gap may be attributed to possible damage of the SiC top surface by irradiation of the high-energy electron beam during the TEM measurement. In turn, this effect may be related to the unstable nature of the SiC top surface, which is terminated by hydrogen atoms but not by the buffer layer consisting of carbon atoms.

Finally, we comment on the key factors for selectively fabricating two different types of TL graphene. We applied the same hydrogenation procedure to both Ar-BL and Vac-BL graphene but obtained two different types of TL graphene with ABA and ABC stacking. This finding indicates that hydrogenation is not related to selective fabrication, and more importantly, the buffer layer is already arranged in the ABA or ABC stacking sequence before hydrogenation. Other parameters observed to control the sample-growth conditions in the present study are temperature and pressure (atmosphere). Ar-BL graphene, which is converted into ABA TL graphene, is prepared at 1510 °C, a much higher temperature than that (1300 °C) for Vac-BL graphene, which transforms into ABC TL graphene. Considering the natural abundance of ABA and ABC portions in natural graphite, it is inferred that the ABA structure is more stable than the ABC one. This difference suggests that the high annealing temperature of Ar-BL graphene is favorable for forming a local atomic arrangement with an ABA stacking sequence, while the low annealing temperature of Vac-BL graphene may lead to a metastable local atomic arrangement with an ABC stacking sequence. Although the environmental effects (Ar atmosphere (ABA sequence) versus high vacuum (ABC)) during annealing are not well understood at present, we think that the terrace size on the sample surface is much larger in Ar-BL graphene than in Vac-BL graphene, as reported in previous studies.[29,30] We infer that the 0.1 MPa Ar atmosphere may exert a certain pressure effect on a graphene sheet during the stacking process. Furthermore, the small terrace size in Vac-BL graphene may favor the formation of less stable ABC TL graphene. To elucidate the mechanism and tune more precisely the growth conditions of TL graphene, it is important to study the structure at the boundary between graphene and the corresponding buffer layer.

In summary, we have reported the first success in the selective fabrication of quasi-free-standing ABA and ABC TL graphene on a SiC substrate. We employed the hydrogen-termination method to convert bilayer graphene with a buffer layer into trilayer graphene. We found that the temperature and pressure (atmosphere) applied in preparing bilayer graphene are the key factors for the selective fabrication. ARPES measurements revealed that ABA graphene possesses a

massless Dirac-cone-like band at the K point, while a parabolic non-Dirac-like band exists at that point in ABC graphene. The present success in the selective fabrication of ABA and ABC TL graphene could enhance the feasibility of fabricating graphene-based nanoelectronic devices with variable layer numbers and stacking sequences.

CONFLICT OF INTEREST

The authors declare no conflict of interest.

ACKNOWLEDGEMENTS

We thank K Suzuki and M Sato for their assistance in the ARPES experiments. This work was supported by JSPS KAKENHI Grant Numbers JP15H02105, JP15H05853, JP25107002 and JP25107003 and the Program for Key Interdisciplinary Research.

Author contributions: NY and KS performed sample growth, data collection, data analysis and ARPES experiments. KM, WN and MK performed TEM experiments. KS, TS and TT conceived the experiments and wrote the paper.

PUBLISHER'S NOTE

Springer Nature remains neutral with regard to jurisdictional claims in published maps and institutional affiliations.

1 Lin, Y.-C., Dumcenco, D. O., Huang, Y.-S. & Suenaga, K. Atomic mechanism of the semiconducting-to-metallic phase transition in single-layered MoS_2. *Nat. Nanotechnol.* **9**, 391–396 (2014).
2 Kappera, R., Voiry, D., Yalcin, S. E., Branch, B., Gupta, G., Mohite, A. D. & Chhowalla, M. Phase-engineered low-resistance contacts for ultrathin MoS_2 transistors. *Nat. Mater.* **13**, 1128–1134 (2014).
3 Cho, S., Kim, S., Kim, J. H., Zhao, J., Seok, J., Keum, D. H., Baik, J., Choe, D.-H., Chang, K. J., Suenaga, K., Kim, S. W., Lee, Y. H. & Yang, H. Phase patterning for ohmic homojunction contact in $MoTe_2$. *Science* **349**, 625–628 (2015).
4 Nakata, Y., Sugawara, K., Shimizu, R., Okada, Y., Han, P., Hitosugi, T., Ueno, K., Sato, T. & Takahashi, T. Monolayer 1*T*-$NbSe_2$ as a Mott insulator. *NPG Asia Mater.* **8**, e321 (2016).
5 Lin, X., Lu, J. C., Shao, Y., Zhang, Y. Y., Wu, X., Pan, J. B., Gao, L., Zhu, S. Y., Qian, K., Zhang, Y. F., Bao, D. L., Li, L. F., Wang, Y. Q., Liu, Z. L., Sun, J. T., Lei, T., Liu, C., Wang, J. O., Ibrahim, K., Leonard, D. N., Zhou, W., Guo, H. M., Wang, Y. L., Du, S. X., Pantelides, S. T. & Gao, H.-J. Intrinsically patterned two-dimensional materials for selective adsorption of molecules and nanoclusters. *Nat. Mater.* **16**, 717–721 (2017).
6 Dresselhaus, M. S. & Dresselhaus, G. Intercalation compounds of graphite. *Adv. Phys.* **51**, 1–186 (2002).
7 Bernal, J. D. The structure of graphite. *Proc. R. Soc. Lond.* **106**, 749 (1924).
8 Haering, R. Band structure of rhombohedral graphite. *Can. J. Phys.* **36**, 352 (1958).
9 Novoselov, K. S., Geim, A. K., Morozov, S. V., Jiang, D., Katsnelson, M. I., Grigorieva, I. V., Dubonos, S. V. & Firsov, A. A. Two-dimensional gas of massless Dirac fermions in graphene. *Nature* **438**, 197–200 (2005).
10 Gorbachev, R. V., Song, J. C. W., Yu, G. L., Kretinin, A. V., Withers, F., Cao, Y., Mishchenko, A., Grigorieva, I. V., Novoselov, K. S., Levitov, L. S. & Geim, A. K. Detecting topological currents in graphene superlattices. *Science* **320**, 206–209 (2008).
11 McCann, E. Asymmetry gap in the electronic band structure of bilayer graphene. *Phys. Rev. B* **74**, 161403R (2006).
12 Oostinga, J. B., Heersche, H. B., Liu, X. L., Morpurgo, A. F. & Vandersypen, L. M. K. Gate-induced insulating state in bilayer graphene devices. *Nat. Mater.* **7**, 151–157 (2007).
13 Koshino, M. Interlayer screening effect in graphene multilayers with ABA and ABC stacking. *Phys. Rev. B* **81**, 125304 (2010).
14 Xiao, R., Tasnadi, F., Koepercik, K., Venderbos, J. W. F., Richter, M. & Taut, M. Density functional investigation of rhombohedral stacks of graphene: topological surface states, nonlinear dielectric response, and bulk limit. *Phys. Rev. B* **84**, 1654004 (2011).
15 Lui, C. H., Li, Z., Mak, K. F., Cappelluti, E. & Heinz, T. F. Observation of an electrically tunable band gap in trilayer graphene. *Nat. Phys.* **7**, 944 (2011).
16 Bao, W., Jing, L., Velasco, J. Jr, Lee, Y., Liu, G., Tran, D., Standley, B., Aykol, M., Cronin, S. B., Smirnov, D., Koshino, M., McCann, E., Bockrath, M. & Lau, C. N. Stacking-dependent band gap and quantum transport in trilayer graphene. *Nat. Phys.* **7**, 948 (2011).
17 Zhang, L., Zhang, Y., Camacho, J., Khodas, M. & Zaliznyak, I. The experimental observation of quantum Hall effect of l = 3 chiral quasiparticles in trilayer graphene. *Nat. Phys.* **7**, 953 (2011).
18 Ohta, T., Bostwick, A., McChesney, J. L., Seyller, T., Horn, K. & Rotenberg, E. Interlayer interaction and electronic screening in multilayer graphene investigated with angle-resolved photoemission spectroscopy. *Phys. Rev. Lett.* **98**, 206802 (2007).
19 Coletti, C., Forti, S., Principi, A., Emtsev, K. V., Zakharov, A. A., Daniels, K. M., Daas, B. K., Chandrashekhar, M. V. S., Ouisse, T., Chaussende, D., MacDonald, A. H., Polini, M. & Starke, U. Revealing the electronic band structure of trilayer graphene on SiC: an angle-resolved photoemission study. *Phys. Rev. B* **88**, 155439 (2013).
20 Bao, C., Yao, W., Wang, E., Chen, C., Avila, J., Asensio, M. C. & Zhou, S. Stacking-dependent electronic structure of trilayer graphene resolved by nanospot angle-resolved photoemission spectroscopy. *Nano Lett.* **17**, 1564–1568 (2017).
21 Ohta, T., Bostwick, A., Seyller, T., Hom, K. & Rotenberg, E. Controlling the electronic structure of bilayer grapheme. *Science* **313**, 951 (2007).
22 Sugawara, K., Sato, T., Kanetani, K. & Takahashi, T. Semiconductor–metal transition and band-gap tuning in quasi-free-standing epitaxial bilayer graphene on SiC. *J. Phys. Soc. Jpn.* **80**, 024705 (2011).
23 Guisinger, N. P., Rutter, G. M., Crain, J. N., First, P. N. & Stroscio, J. A. Exposure of epitaxial graphene on SiC(0001) to atomic hydrogen. *Nano Lett.* **9**, 1462–1466 (2009).
24 Riedl, C., Coletti, C., Iwasaki, T., Zakharov, A. A. & Starke, U. Quasi-free-standing epitaxial graphene on SiC obtained by hydrogen intercalation. *Phys. Rev. Lett.* **103**, 246804 (2009).
25 Avetisyan, A. A., Partoens, B. & Peeters, F. M. Electric field tuning of the band gap in graphene multilayers. *Phys. Rev. B* **79**, 035401 (2009).
26 Avetisyan, A. A., Partoens, B. & Peeters, F. M. Stacking order dependent electric field tuning of the gap in graphene multilayers. *Phys. Rev. B* **81**, 115432 (2010).
27 Charlier, J. -C., Gonze, X. & Micheanud, J. -P. First-principles study of the stacking effect on the electronic properties of gphite. *Carbon* **32**, 289–299 (1994).
28 Norimatsu, W. & Kusunoki, M. Selective formation of ABC-stacked graphene layers on SiC(0001). *Phys. Rev. B* **81**, 161410R (2010).
29 Zhou, S., Siegel, D. A., Fedorov, A. V., Gabaly, F. El, Schmid, A. K., Castro Neto, A. H., Lee, D. -H. & Lanzara, A. Origin of the energy band gap in epitaxial graphene. *Nat. Mater.* **7259** (2008).
30 Emtev, K. V., Bostwick, A., Horn, K., Jobst, J., Kellogg, G. L., Ley, L., McChesney, J. L., Ohta, T., Reshanov, S. A., Röhrl, J., Rotenberg, E., Schmid, A. K., Waldmann, D., Weber, H. B. & Seyller, T. Towards wafer-size graphene layers by atmospheric pressure graphitization of silicon carbide. *Nat. Mater.* **8**, 203 (2009).